

Supplementary Information:

A novel strategy for fabricating highly stretchable and highly conductive photoluminescent ionogels via in situ self-catalytic cross- linking reaction in ionic liquids

*Shuai Hao,^a Jianxin Zhang,^a Xuemeng Yang,^a Tianci Li,^a Hongzan Song^{*a}*

^aCollege of Chemistry & Environmental Science, Hebei University, Baoding, Hebei

Province 071002, P. R. China

*Corresponding Author:

E-mail: songhongzan@iccas.ac.cn (H. S.)

Experimental section

Materials

1-vinyl-3-butylimidazolium tetrafluoroborate (VBIMBF₄) and 1-vinyl-3-butylimidazolium hexafluorophosphate (VBIMPF₆) have been purchased from Shanghai Cheng Jie Chemical Co. LTD. 1-butyl-3-methylimidazolium tetrafluoroborate (BMIMBF₄), 1-butyl-3-methylimidazolium hexafluorophosphate (BMIMPF₆), glycidyl methacrylate (GMA), and 2-Hydroxy-4'-(2-hydroxyethoxy)-2-methylpropiophenone (photoinitiator) have been purchased from Sigma-Aldrich. Note that all ionic liquids should be dried at 80 °C in vacuum for 48 h prior to use.

Synthesis of Ionogels

Firstly, the raw materials of VBIMBF₄, glycidyl methacrylate and photoinitiator were dissolved in BMIMBF₄ under magnetic stirring for 2 h at 25 °C to obtain a homogenous solution. Then the above solutions were exposed under an ultraviolet exposure chamber. After being irradiated for 2 h (wavelength of 365 nm), homogenous poly(ionic liquid) copolymers/ionic liquid solutions were obtained. Then the obtained solutions were allowed to heat for 2 h and the ionogels were obtained. Note that all the ionogels were prepared in a glovebox under nitrogen atmosphere. The samples based on ionic liquid monomer VBIMPF₆ and ionic liquid BMIMPF₆ were also prepared. The structures of the used raw materials (ionic liquids, ionic liquid monomers, and epoxy monomer) and the reaction scheme are shown in Figure 1. The proposed mechanism of poly(ionic liquid)/epoxy resin copolymer cross-linking with ILs as catalysts is shown in Fig. 1. The composition of the ionogels is shown in Table S1.

Characterization

Rheological measurements were measured by a stress-controlled rheometer (TA-AR2000EX) with 25 mm diameter parallel-plate geometry. Fourier Transform infrared spectroscopy (FTIR) spectra were recorded on a Varian-640 spectrophotometer. Microstructure of the ionogels was observed by JEOL SEM 6700.

Mechanical performance was measured by Linkam LINKSYS 32 tensile hot stage (Linkam, UK) and the rate is 0.2 mm/min. The curing process of ionogels was investigated using DSC Q800 (TA Instruments). Fluorescence spectra were measured by a fluorescence spectrometer (RF-5301pc, Shimadzu) with slit width of 10 nm for both the excitation and emission. Fluorescence quantum yield and the average fluorescence lifetime of the ionogel were measured by a fluorescence spectrometer (FLS980, Edinburgh) connected with an integrating sphere. The fluorescence of ionogels was measured by a ZEISS Axio Vert.A1 fluorescence microscope. Resistances of the ionogels were measured using a Zahner IM6e electrochemical workstation (Zahner, Germany) over the frequency range from 1Hz to 500 kHz at an AC oscillation of 10mV. Ionic conductivities were calculated from the resistances obtained from the impedance spectra. The minimum in the Nyquist plot of the negative imaginary part of the impedance versus the real part of the impedance was taken as the sample resistance, R . The ionic conductivity, σ , was calculated as $d/(RS)$, where d and S are the thickness and area of the sample, respectively. The measurements of the samples, having a diameter of 8mm and thickness of 2mm, were carried out in a cell, which consisted of a Teflon spacer sandwiched between two platinum coated stainless steel electrodes. Keithley DMM7510 system electrometer with Linkam TST 350 tensile hot stage was used to measure the electromechanical performances of the strain sensor.

Table S1 Composition of the prepared ionogels

Samples	BMIMBF₄/wt%	GMA+VBIMBF₄/wt%	CMA: VBIMBF₄
60%-BMIMBF₄-1	60	40	1:5
60%-BMIMBF₄-2	60	40	1:7
60%-BMIMBF₄-3	60	40	1:10
60%-BMIMBF₄-4	60	40	1:12
65%-BMIMBF₄-1	65	35	1:5
65%-BMIMBF₄-2	65	35	1:6
65%-BMIMBF₄-3	65	35	1:7
65%-BMIMBF₄-4	65	35	1:10
70%-BMIMBF₄-1	70	30	1:3
70%-BMIMBF₄-2	70	30	1:5
70%-BMIMBF₄-3	70	30	1:7
70%-BMIMBF₄-4	70	30	1:10

Table S2 Comparison between this work and previously-reported stretchable chemical ionogels.

Polymer network	Cross-linker	Stretchability	Temperature tolerance (°C)	Conductivity at 25 °C (mS/cm)	Devices	Refs.
PIL network	No	~1200%	-40-200	>1	Sensor	This work
PIL network	Hyperbranched polymer	~1000%	-60-250	5.8	Sensor	42
F127DA network	F127DA	~250%	Not shown	0.1-1	Sensor	26
PAA network	PEGDA	~2000%	-20-80	1	Sensor	30
PBA network.	PEGDA	~700%	-30-100	~0.1	Sensor	31
PAA network	F127DA	~850%	-28-100	19	Sensor	27

Table S3. Compare the conductivity between this work and previously-reported ionogels.

Polymer network	Conductivity at 25 °C (mS/cm)	Refs.
PIL	>1	This work
F127DA	0.1-1	26
PBA	~0.1	31
PVDF-co-HFP	0.01-0.1	32
P(VDF-HFP)	0.8	69

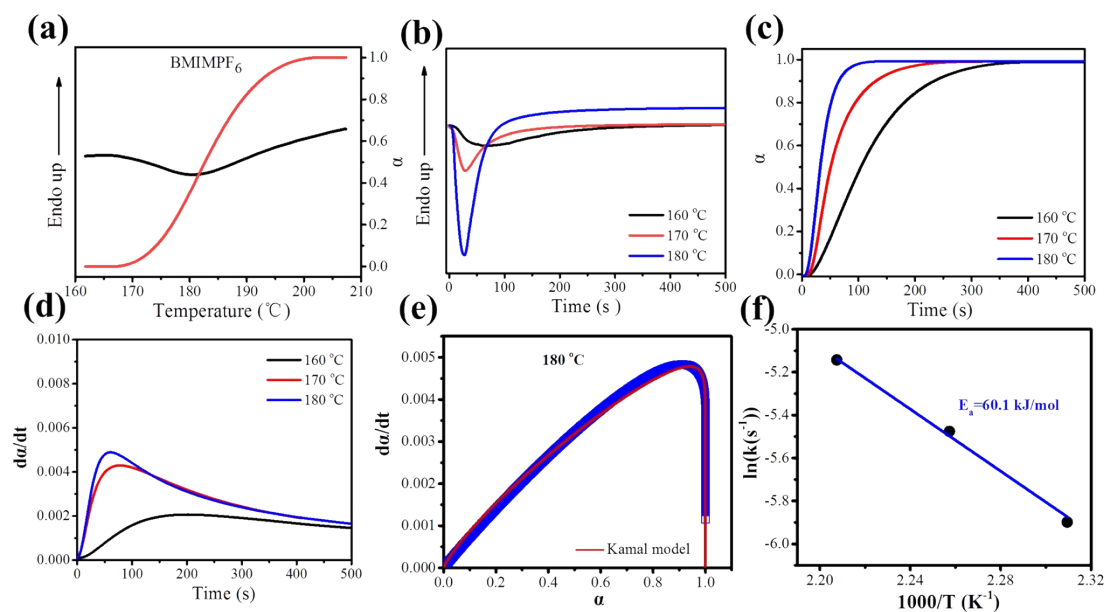


Fig. S1 (a) DSC curves of heating scans for the poly(VBIMPF₆)/epoxy resin copolymer/BMIMPF₆ solutions at a heating rate of 10 °C/min. (b) Heat flow versus time for isothermal cure of the poly(VBIMPF₆)/epoxy resin copolymer/BMIMPF₆ solutions at different temperatures. (c) Time evaluations of DSC conversion for BMIMBF₆ system cured at different temperatures. (d) The change of da/dt with time. (e) The change of da/dt with α . Solid red line present a fitting line with Kamal model. (e) Temperature dependence of the constant rates.

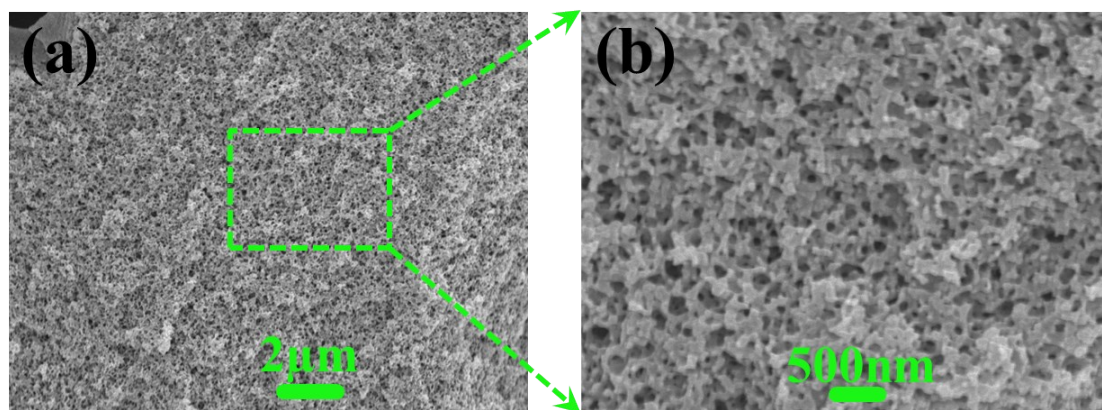


Fig. S2 SEM images of (a) and (b) cross-sections of ionogels based on poly(VBIMPF₆)/epoxy resin copolymer.

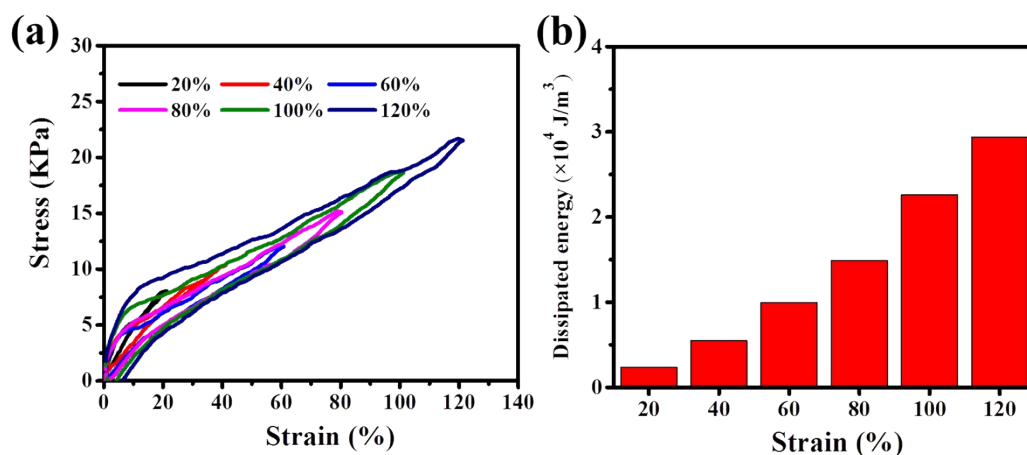


Fig. S3 (a) Stress-strain curves of ionogel during cyclic loading-unloading. (b) Dissipated energy in (a).

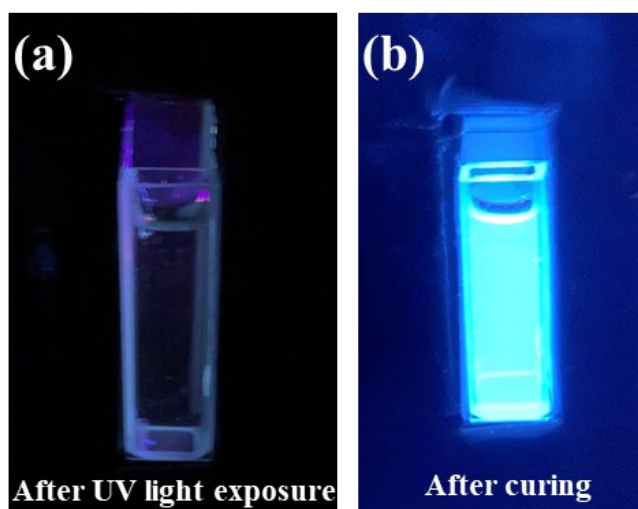


Fig. S4 Fluorescence images of the samples (UV light, 365 nm): (a) After UV light exposure (solution). (b) After curing (gel).

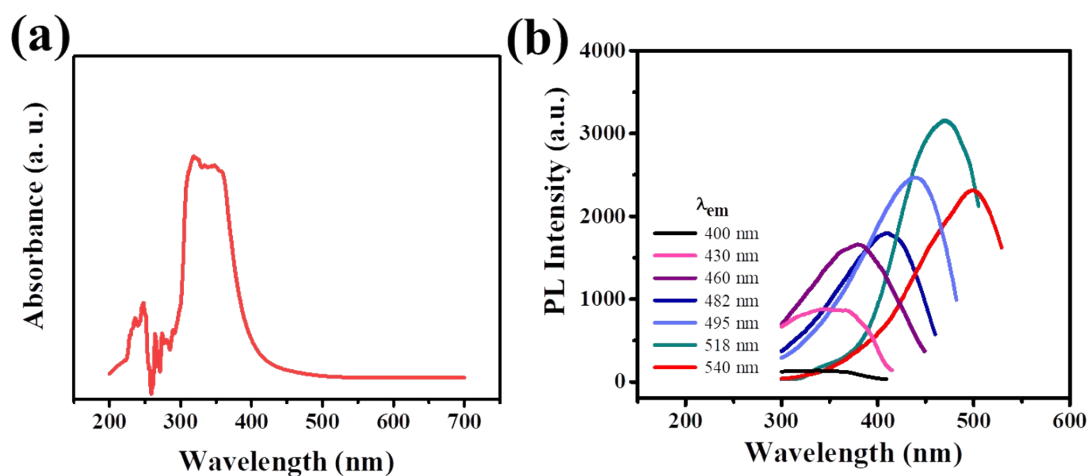


Fig. S5 (a) UV-vis absorption spectra of ionogel. (b) Photoluminescence excitation spectra of ionogel.

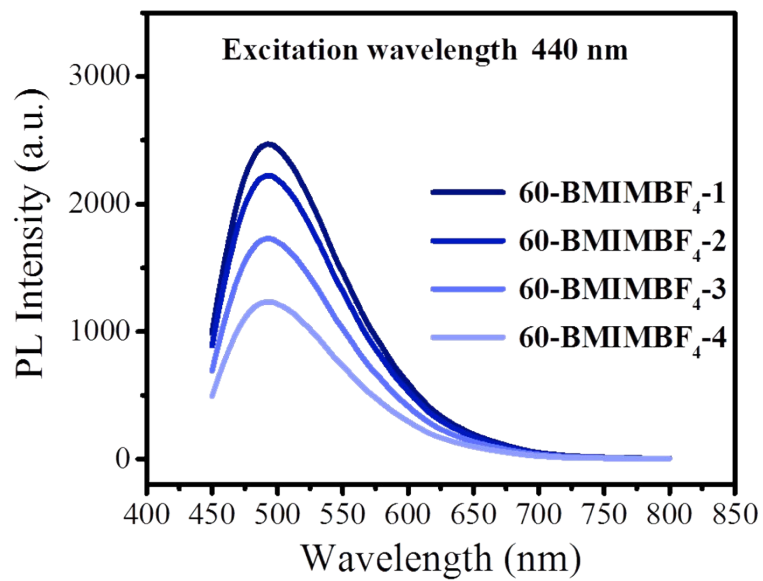


Fig. S6 Excitation-dependent photoluminescence of ionogels with different content of GMA at excitation wavelength 440 nm.

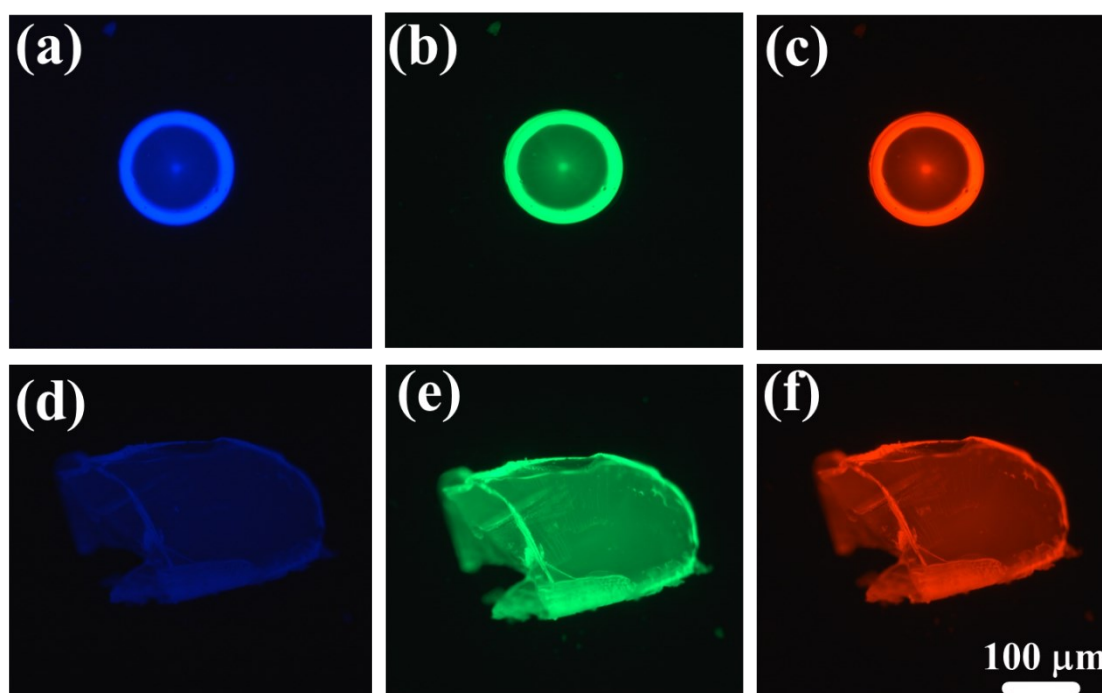


Fig. S7 (a)-(f) Fluorescence images of as-prepared ionogels (after removing ionic liquid) under varied excitation wavelengths (380-405, 440-490, and 510-550 nm).



Fig. S8 Fluorescence images of the neat PIL, PIL/EP, and neat EP (UV light, 365 nm).

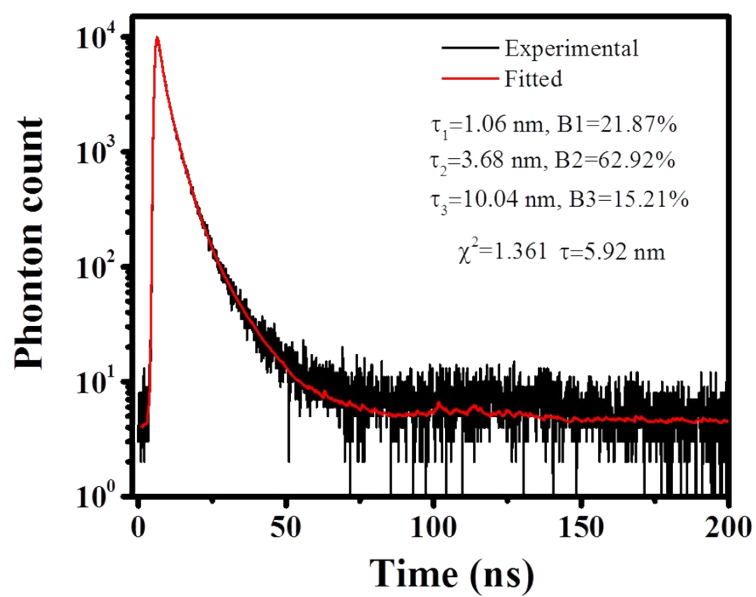


Fig. S9 Average fluorescence lifetime of the ionogel that excited at 470 nm.

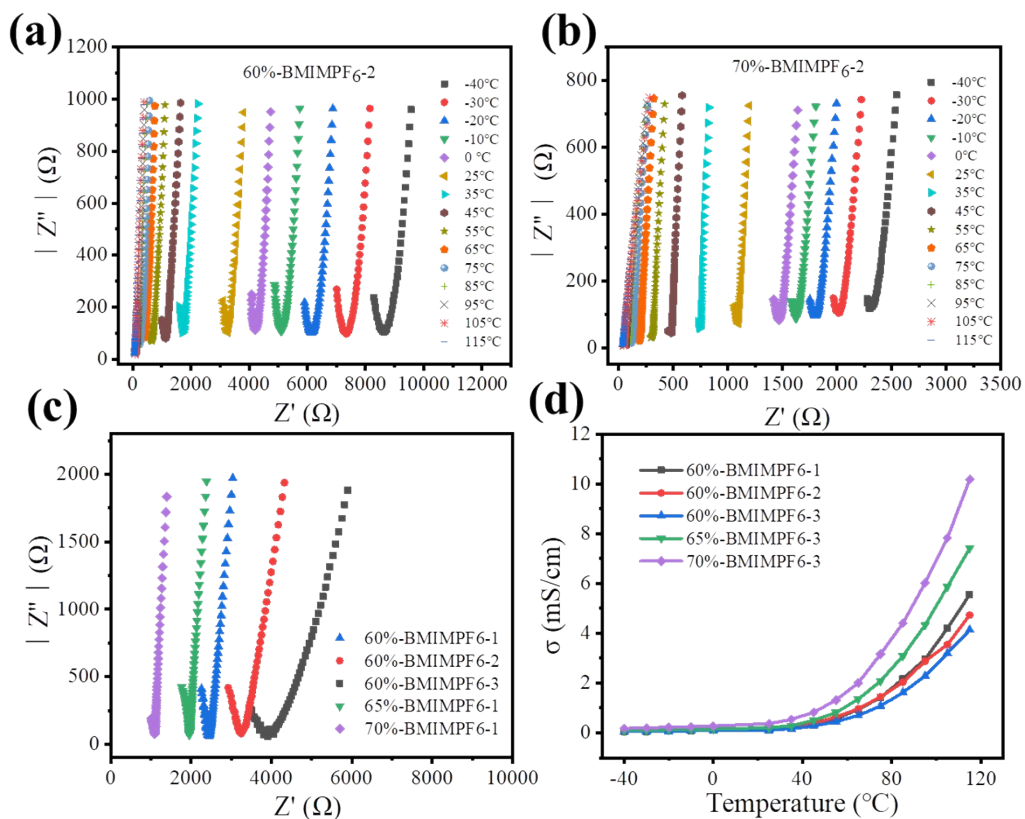


Fig. S10 The impedance plots: (a) 60%-BMIMPF₆-2 ionogel at different temperatures; (b) 70%-BMIMPF₆-2 ionogel at different temperatures; (c) Ionogels with different content of polymers and ionic liquid (25 °C). (d) Temperature dependence of ionic conductivities for ionogels.

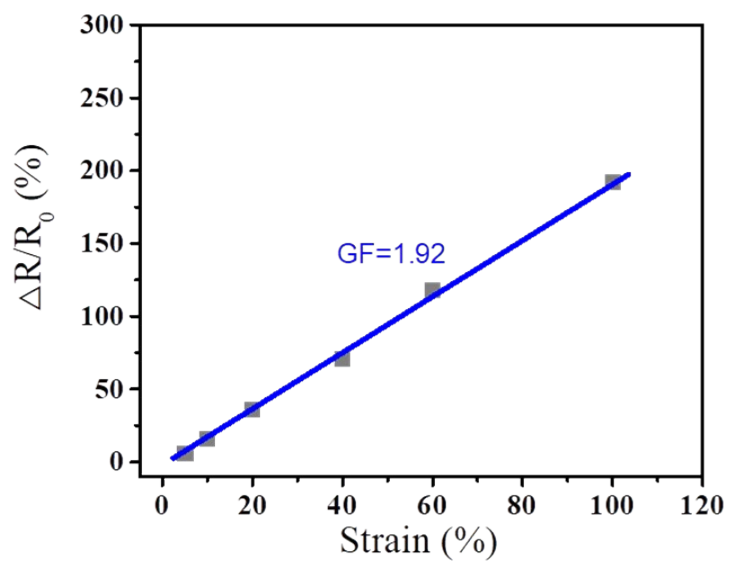


Fig. S11 $\Delta R/R_0$ variation of the sensor with different strain.

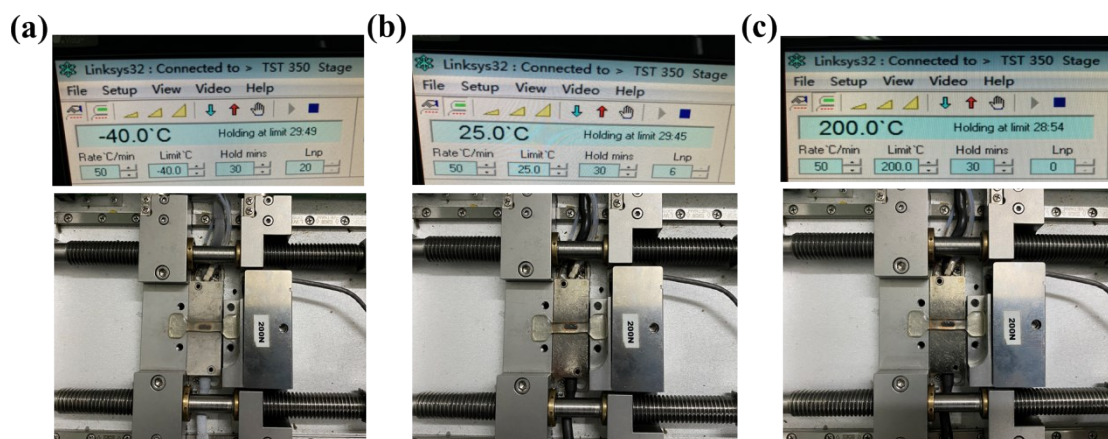


Fig. S12 (a)-(c) The dimensional stability of the ionogel sample under different temperature.